Polymer chains in confined geometries: Massive field theory approach

D. Romeis
Leibniz Institute for Polymer Research Dresden eV, 01069 Dresden, Germany

Z. Usatenko
Institute for Condensed Matter Physics, National Academy of Sciences of Ukraine, 79011 Lviv, Ukraine

(Received 27 April 2009; published 7 October 2009)

The massive field theory approach in fixed space dimensions $d<4$ is applied to investigate a dilute solution of long-flexible polymer chains in a good solvent between two parallel repulsive walls, two inert walls, and for the mixed case of one inert and one repulsive wall. The well-known correspondence between the field theoretical ϕ^4 $O(n)$-vector model in the limit $n\to 0$ and the behavior of long-flexible polymer chains in a good solvent is used to calculate the depletion interaction potential and the depletion force up to one-loop order. In order to make the theory UV finite in renormalization-group sense in $3\leq d<4$ dimensions we performed the standard mass renormalization and additional surface-enhancement constants renormalization. Besides, our investigations include modification of renormalization scheme for the case of two inert walls. The obtained results confirm that the depletion interaction potential and the resulting depletion force between two repulsive walls are weaker for chains with excluded volume interaction (EVI) than for ideal chains because the EVI effectively reduces the depletion effect near the walls. Our results are in qualitative agreement with previous theoretical investigations, experimental results, and with the results of Monte Carlo simulations.

DOI: 10.1103/PhysRevE.80.041802 PACS number(s): 61.25.he, 64.60.fd, 68.35.Md, 82.70.Dd

I. INTRODUCTION

Solutions of long flexible polymer chains in confined geometries such as thin films, porous media, or mesoscopic particles dissolved in the solution have been extensively studied in recent years, including experimental, numerical, and theoretical investigations. These investigations showed that polymer solutions and binary liquid mixture in confined geometries give rise to new phenomena not observed in bulk. In general, macroscopic bodies immersed in a medium frequently feel long-range forces originating from fluctuations in the medium. Such fluctuation-induced forces are omnipresent in nature. For example, such forces arise as a result of the confinement of quantum fluctuations of the electromagnetic field between two metallic conducting plates and due to the well-known quantum-electrodynamic Casimir effect [1]. The confinement of thermal fluctuations of the order parameter at critical points in a binary liquid mixture leads to effective long-range forces between the confining walls or particles immersed in fluid as it was predicted by Fisher and de Gennes [2]. They are commonly known as critical (or thermodynamic) Casimir forces. Such thermodynamic Casimir forces were recently verified experimentally by their direct observation in binary fluid mixtures [3]. In polymer solutions, the reason for these forces originates from the presence of depletion zones near the confining walls or mesoscopic particles due to an additional amount of entropic energy for polymers confined within the slit or between colloidal particles. For entropic reasons, the polymer chains avoid the space between the walls or two close particles. It leads to an unbalanced pressure the outside which pushes the two walls or two colloidal particles towards each other. The improvement of the experimental technique recently allowed even to measure with high accuracy the depletion force between a wall and a single colloidal particle [3–6]. It should be mentioned that the case of two parallel walls gives the possibility, via the Derjaguin approximation [7], to describe the case of a big colloidal spherical particle near the wall when the radius of particle R is larger than the radius of gyration R_g and exceeds the distance between the particle and the wall L.

During a long period the interaction between polymers and colloidal particles has been modeled by approximating the polymer chains as hard spheres [8,9]. But such an approach does not make it possible to correctly describe the behavior of small colloidal particles in polymer solution and in the case of colloidal particles of big size the difference between theoretical predictions and experimental data is bigger than 10%. In accordance with this, the approaches which take into account the chain flexibility were more effective. For example, in the case of strongly overlapping polymer chains (semidilute solutions), the chain flexibility was taken into account via the phenomenological scaling theory [10,11] or the self-consistent field theory [12]. In the case of dilute polymer solution, different polymer chains do not overlap and the behavior of such polymer solution can be described by a single polymer chain using the model of random walk (RW) (for the ideal chain at θ-solvent) or self-avoiding walk (for the real polymer chain with excluded volume interaction). The latter case corresponds to the situation when the solvent temperature is above the θ-point (good solvent) and the polymer coils are less compact than in the case of ideal chains. A remarkable progress in the investigation of this task was achieved by [13,14] via using a dimensionally regularized continuum version of the field theory with minimal subtraction of poles in $\epsilon=4-d$, where d is dimensionality of space. But, as it is easy to see [14], still there are a lot of unsolved problems and the question arises: "how to find a theory which allows us to explain experimental data in a better way?" One of the methods, which up to our knowledge has not yet been applied to this task, is the massive field theory approach. This method, as it was shown in the case of

infinite [15,16], semi-infinite [17] systems, and specially in the case of dilute polymer solutions in semi-infinite geometry [18] gives better agreement with the experimental data and the results of Monte Carlo (MC) calculations. In accordance with this, the purpose of the present work is to apply the massive field theory approach in fixed space dimension $d=3$ for the investigation of dilute polymer solution within the slit of two parallel walls being in equilibrium contact with an equivalent polymer solution in a reservoir outside the slit and to calculate the depletion interaction potentials and the depletion forces which arise in a system.

The most remarkable properties of fluctuation-induced forces is their universality. They are independent of most microscopic details and depend only on a few macroscopic properties such as the adsorption properties of the confining walls or the shape of the particles. In accordance with this, we used different combinations of confining walls, i.e., we performed calculations for the case of two repulsive walls, two inert walls, and a mixed case of one repulsive and one inert wall. Besides, taking into account the Derjaguin approximation [7] we obtained results for colloidal particles of big radius near the wall and compared the obtained results with the experimental data [5]. In the case of two repulsive walls we found good agreement of our results with the results of Monte Carlo simulations [19,20].

II. MODEL

We shall assume that the solution of polymer chains is sufficiently dilute so that the interchain interactions and the overlapping between different chains can be neglected, and it is sufficient to consider the configurations of a single chain. Long flexible polymer chains in a good solvent are perfectly described by the model of self-avoiding walks (SAWs) on a regular lattice [21,22]. Taking into account the polymer-magnet analogy developed by [23], their scaling properties in the limit of an infinite number of steps N may be derived by a formal $n\to 0$ limit of the field theoretical ϕ^4 $O(n)$-vector model at its critical point. The average square end-to-end distance, the number of configurations with one end fixed and with both ends fixed at the distance $x=\sqrt{(\vec{x}_A-\vec{x}_B)^2}$ exhibit the following asymptotic behavior in the limit $N\to\infty$:

$$\langle R^2\rangle \sim N^{2\nu}, \quad Z_N \sim q^N N^{\gamma-1}, \quad Z_N(x) \sim q^N N^{-(2-\alpha)}, \tag{2.1}$$

respectively. ν, γ, and α are the universal correlation length, susceptibility, and specific heat critical exponents for the $O(n)$ vector model in the limit $n\to 0$, d is the space dimensionality, and q is a nonuniversal fugacity. $1/N$ plays the role of a critical parameter analogous to the reduced critical temperature in magnetic systems.

In the case when the polymer solution is in contact with a solid substrate, the monomers interact with the surface. At temperatures, $T<T_a$, the attraction between the monomers and the surface leads to a critical adsorbed state, where a finite fraction of the monomers is attached to the wall and form $d-1$ dimensional structure. The deviation from the adsorption threshold $[c\propto(T-T_a)/T_a]$ changes sign at the transition between the adsorbed (the so-called normal transition, $c<0$) and the nonadsorbed state (ordinary transition, $c>0$), and it plays the role of a second critical parameter. The value c corresponds to the adsorption energy divided by k_BT (or the surface-enhancement constant in field theoretical treatment). It should be mentioned that for the sake of convenience we prefer to use the field theoretical terminology for constant c throughout the whole of the paper. The adsorption threshold for long-flexible infinite polymer chains, where $1/N\to 0$ and $c\to 0$ is a multicritical phenomenon.

The aim of the present investigations is to describe the behavior of such dilute solution of long-flexible polymer chains within the slit of two parallel walls which is in equilibrium contact with an equivalent polymer solution in a reservoir outside the slit. The walls are located at the distance L one from another in z direction such that the surface of the bottom wall is located at $z=0$ and the surface of the upper wall is located at $z=L$. Each of the two surfaces of the system is characterized by a certain surface-enhancement constant c_i, where $i=1,2$. The effective Landau-Ginzburg Hamiltonian describing the system of dilute polymer solution confined to the slit is

$$\mathcal{H}_{\|}[\vec{\phi}] = \int d^{d-1}r \int_0^L dz \left\{ \frac{1}{2}(\nabla\vec{\phi})^2 + \frac{1}{2}\mu_0^2\vec{\phi}^2 + \frac{1}{4!}v_0(\vec{\phi}^2)^2 \right\} + \frac{c_{1_0}}{2}\int d^{d-1}r\vec{\phi}^2(\mathbf{r},z=0) + \frac{c_{2_0}}{2}\int d^{d-1}r\vec{\phi}^2(\mathbf{r},z=L), \tag{2.2}$$

where $\vec{\phi}(\mathbf{x})$ is an n-vector field with the components $\phi_i(x)$, $i=1,\ldots,n$ and $\mathbf{x}=(\mathbf{r},z)$, μ_0 is the "bare mass," and v_0 is the bare coupling constant which characterizes the strength of the excluded volume interaction (EVI). The surfaces introduce an anisotropy into the problem, and the directions parallel and perpendicular to the surfaces are no longer equivalent. In accordance with the fact that we have to deal with slit geometry $[\mathbf{x}=(\mathbf{r},0\le z\le L)]$, only parallel to surfaces Fourier transforms in $d-1$ dimensions take place. The interaction between the polymer chain and the walls is implemented by the different boundary conditions. As it was mentioned above, we consider the case of two repulsive walls, where the fields $\vec{\phi}(\mathbf{r},z)$ satisfy Dirichlet-Dirichlet boundary conditions

$$c_1\to+\infty, \quad c_2\to+\infty \quad or \quad \vec{\phi}(\mathbf{r},0)=\vec{\phi}(\mathbf{r},L)=0, \tag{2.3}$$

two inert walls (Neumann-Neumann boundary conditions)

$$c_1=0, \quad c_2=0 \quad or \quad \left.\frac{\partial\vec{\phi}(\mathbf{r},z)}{\partial z}\right|_{z=0} = \left.\frac{\partial\vec{\phi}(\mathbf{r},z)}{\partial z}\right|_{z=L} = 0, \tag{2.4}$$

and the mixed case of one repulsive and one inert wall (Dirichlet-Neumann boundary conditions)

$$c_1 \to +\infty, \quad c_2 = 0 \quad or \quad \vec{\phi}(\mathbf{r},0) = 0, \qquad \left.\frac{\partial \vec{\phi}(\mathbf{r},z)}{\partial z}\right|_{z=L} = 0. \tag{2.5}$$

The requirement in Eq. (2.4) describing the inert character of the walls corresponds to the fixed point of the so-called special transition [17,24,25] in the field theoretical treatment.

In the present case, the only relevant lengths are the average end-to-end distance $\xi_R = \sqrt{\langle R^2 \rangle} \sim N^{\nu}$ and the length L—the distance between two walls. The properties of the system depend on the ratio L/ξ_R. It should be mentioned that the present field-theoretical approach is not able to describe the dimensional crossover from d to $d-1$-dimensional systems which arises for $L \ll \xi_R$. In this case the system is characterized by another critical temperature (see, for example, on the situation in magnetic or liquid thin films) and moves to a new critical fixed point.

Thus the present theory is valid for the case $L \gg \xi_R$. Nevertheless, we made some assumptions, which allowed us to describe the region $L \ll \xi_R$.

The well-known arguments of the polymer-magnet analogy [21–23,26] assume the correspondence between the partition function $Z_{\parallel}(\mathbf{x},\mathbf{x}')$ of polymer chain with ends fixed at $\mathbf{x}$ and $\mathbf{x}'$ immersed in the volume containing the two parallel walls and the two-point correlation function $G^{(2)}(\mathbf{x},\mathbf{x}') = \langle \vec{\phi}(\mathbf{x}) \vec{\phi}(\mathbf{x}') \rangle$ in the field theoretical ϕ^4 $O(n)$-vector model at the formal limit $n \to 0$ in the restricted geometry:

$$Z_{\parallel}(\mathbf{x},\mathbf{x}';N,L,v_0) = \mathcal{IL}_{\mu_0^2 \to N}[\langle \vec{\phi}_1(\mathbf{x}) \vec{\phi}_1(\mathbf{x}') \rangle|_{n=0}]. \tag{2.6}$$

Here the rhs denotes the inverse Laplace transform $\mu^2 \to N$ of the two-point correlation function for the system modeled via the corresponding Landau-Ginzburg Hamiltonian in the limit, where the number of components n tends to zero. N determines the number of monomers of the polymer chain and represents only an auxiliary parameter, the trace along the chain and fixes its *size* globally. The most common parameter in polymer physics to denote the size of polymer chains which are observable in experiments is R_g [21,22,26]:

$$R_g^2 = \chi_d^2 \frac{R_x^2}{2}, \tag{2.7}$$

where χ_d is a universal numerical prefactor which depends on the dimension d of the system. For ideal polymer chains one has $\chi_d^2 = \frac{d}{3}$ and for three dimensional case N equals $R_x^2/2$. For the chains with EVI it could be obtained within a perturbation expansion [21].

The fundamental two-point correlation function of the free theory corresponding to Eq. (2.2) in mixed $\mathbf{p},z$ representation has a form

$$\tilde{G}_{ij}^{(2)}(\mathbf{p},\mathbf{p}',z,z') = (2\pi)^{d-1} \delta_{ij} \delta(\mathbf{p}+\mathbf{p}') \tilde{G}_{\parallel}(\mathbf{p},z,z';\mu_0,c_{1_0},c_{2_0},L), \tag{2.8}$$

where the free propagator $\tilde{G}_{\parallel}(\mathbf{p},z,z';\mu_0,c_{1_0},c_{2_0},L)$ of model (2.2) is

$$\begin{aligned}
&\tilde{G}_{\parallel}(\mathbf{p},z,z';\mu_0,c_{1_0},c_{2_0},L) \\
&= \frac{1}{2\kappa_0}\{[\kappa_0^2 + \kappa_0(c_{1_0}+c_{2_0}) + c_{1_0}c_{2_0}]e^{\kappa_0 L} \\
&\quad - [\kappa_0^2 - \kappa_0(c_{1_0}+c_{2_0}) + c_{1_0}c_{2_0}]e^{-\kappa_0 L}\}^{-1} \\
&\quad \times \{[\kappa_0^2 + \kappa_0(c_{1_0}+c_{2_0}) + c_{1_0}c_{2_0}]e^{\kappa_0(L-|z-z'|)} \\
&\quad + [\kappa_0^2 - \kappa_0(c_{1_0}+c_{2_0}) + c_{1_0}c_{2_0}]e^{-\kappa_0(L-|z-z'|)} \\
&\quad + [\kappa_0^2 + \kappa_0(c_{2_0}-c_{1_0}) - c_{1_0}c_{2_0}]e^{\kappa_0(L-z-z')} \\
&\quad + [\kappa_0^2 - \kappa_0(c_{2_0}-c_{1_0}) - c_{1_0}c_{2_0}]e^{-\kappa_0(L-z-z')}\},
\end{aligned} \tag{2.9}$$

with $\kappa_0 = \sqrt{p^2+\mu_0^2}$, where $\mathbf{p}$ is the value of parallel momentum associated with $d-1$ translationally invariant directions in the system and the subscript 0 on c_{i_0} (with $i=1,2$) is introduced to avoid confusion with the later defined renormalized variable c_i. At the confining surfaces, the two-point correlation function [Eq. (2.8)] obeys the boundary conditions:

$$\frac{\partial}{\partial z}\tilde{G}_{ij}^{(2)}(\mathbf{p},\mathbf{p}',z,z')|_{z=0} = c_{1_0}\tilde{G}_{ij}^{(2)}(\mathbf{p},\mathbf{p}',z=0,z'),$$

$$\frac{\partial}{\partial z}\tilde{G}_{ij}^{(2)}(\mathbf{p},\mathbf{p}',z,z')|_{z=L} = c_{2_0}\tilde{G}_{ij}^{(2)}(\mathbf{p},\mathbf{p}',z=L,z'). \tag{2.10}$$

In the particular cases of the above-mentioned boundary conditions (Dirichlet-Dirichlet, Neumann-Neumann or Dirichlet-Neumann) the propagator [Eq. (2.9)] reduces to the free propagators noted in [27] (see also Appendix A).

In the case $L \to \infty$ and $0 \le z,z' \ll L$ (or $0 \ll z,z' \le L$) the free propagator [Eq. (2.9)] reproduces the free propagator of the semi-infinite model (see [17] and Appendix B) with the corresponding surface at $z=0$ and the surface-enhancement constant c_{1_0} (or at $z=L$ with c_{2_0}). Thus, for infinitely large wall separations, the slit system decomposes into two half-space (HS) systems.

III. THERMODYNAMIC DESCRIPTION

We consider the dilute solution of long-flexible polymer chains within the slit and allow the exchange of polymer coils between the slit and the reservoir. Thus the polymer solution in the slit is in equilibrium contact with an equivalent solution in the reservoir. We follow the thermodynamic description of the problem as given in [14]. The free energy of the interaction between the walls in such a grand canonical ensemble is defined as the difference of the free energy of an ensemble where the separation of the walls is fixed at a finite distance L and that where the walls are separated infinitely far from each other:

$$\delta F = -k_B T \mathcal{N} \ln\left(\frac{\mathcal{Z}_\parallel(L)}{\mathcal{Z}_\parallel(L\to\infty)}\right) = -k_B T \mathcal{N}\left\{\ln\left(\frac{\mathcal{Z}_\parallel(L)}{\mathcal{Z}}\right) - \ln\left(\frac{\mathcal{Z}_\parallel(L\to\infty)}{\mathcal{Z}}\right)\right\}, \quad (3.1)$$

where $\mathcal{N}$ is the total amount of polymers in the solution and T is the temperature. $\mathcal{Z}_\parallel(L)$ is the partition function of one polymer chain located in volume V containing the walls at a distance L:

$$\mathcal{Z}_\parallel(L) = \int_V \int_V d^d x d^d x' \mathcal{Z}_\parallel(\mathbf{x},\mathbf{x}'), \quad (3.2)$$

with $\mathcal{Z}_\parallel(\mathbf{x},\mathbf{x}')$ representing the partition function of one polymer chain in the slit with its ends fixed at points $\mathbf{x}$ and $\mathbf{x}'$. For the sake of convenience we renormalized the partition functions $\mathcal{Z}_\parallel(L)$ and $\mathcal{Z}_\parallel(L\to\infty)$ on the partition function Z of one polymer chain in the same volume V without walls. The total volume of the system V can be divided into two independent subsystems V_i (inside) and V_o (outside) the slit, respectively. It gives the possibility to expand the term $\ln(\mathcal{Z}_\parallel/\mathcal{Z})$ in the thermodynamic limit as

$$\frac{1}{V}\int_{V_o} d^d x \left(\frac{\hat{\mathcal{Z}}_o(z)}{\hat{\mathcal{Z}}_b} - 1\right) + \frac{1}{V}\int_{V_i} d^d x \left(\frac{\hat{\mathcal{Z}}_i(z)}{\hat{\mathcal{Z}}_b} - 1\right), \quad (3.3)$$

with $\mathcal{Z} = V\hat{\mathcal{Z}}_b$, $\hat{\mathcal{Z}}_b = \int_V d^d x' \mathcal{Z}_b(\mathbf{x},\mathbf{x}')$, where $\mathcal{Z}_b(\mathbf{x},\mathbf{x}')$ is the partition function of one polymer chain in the unbounded solution with fixed ends at $\mathbf{x}$ and $\mathbf{x}'$, and $\hat{\mathcal{Z}}_{o,i}(z) = \int_{V_{o,i}} d^d x' \mathcal{Z}_\parallel(\mathbf{x},\mathbf{x}')$.

In the thermodynamic limit (as $\mathcal{N}, V\to\infty$) the contribution from the first term in Eq. (3.3) and, respectively, in Eq. (3.1) disappear because the ratio $\hat{\mathcal{Z}}_o(z)/\hat{\mathcal{Z}}_b$ is independent of L. Thus, *the reduced free energy of interaction* δf per unit area $A=1$ of the confining walls may be written as

$$\delta f = \frac{\delta F}{n_p k_B T} = L - \int_{V_i} d^d x \frac{\hat{\mathcal{Z}}_i(z)}{\hat{\mathcal{Z}}_b} + \int_{V_{HS_1}} d^d x \left(\frac{\hat{\mathcal{Z}}_{HS_1}(z)}{\hat{\mathcal{Z}}_b} - 1\right) + \int_{V_{HS_2}} d^d x \left(\frac{\hat{\mathcal{Z}}_{HS_2}(z)}{\hat{\mathcal{Z}}_b} - 1\right), \quad (3.4)$$

where $n_p = \mathcal{N}/V$ is the number density of polymer chains in the bulk solution and

$$\hat{\mathcal{Z}}_{HS_i}(z) = \int_{V_{HS}} d^d x' \mathcal{Z}_{HS_i}(\mathbf{x},\mathbf{x}'), \quad (3.5)$$

with $i=1,2$ and $\mathcal{Z}_{HS_i}(\mathbf{x},\mathbf{x}')$ denoting the corresponding partition functions for a polymer chain in a half space with two fixed ends at points $\mathbf{x}$ and $\mathbf{x}'$. The functions $\hat{\mathcal{Z}}_i(z)$ and $\hat{\mathcal{Z}}_{HS_i}(z)$ depend only on the z coordinates perpendicular to walls. The reduced free energy of interaction δf, according to Eq. (3.4), is a function of the dimension of a length and dividing it by another relevant length scale (namely, that for the size of the chain in bulk, e.g., R_x) yields a universal dimensionless scaling function

$$\Theta(y) = \frac{\delta f}{R_x}, \quad (3.6)$$

where $y = L/R_x$ is a dimensionless scaling variable. The resulting depletion force between the two walls induced by the polymer solution is denoted as

$$\Gamma(y) = -\frac{d(\delta f)}{dL} = -\frac{d\Theta(y)}{dy}. \quad (3.7)$$

According to Eqs. (3.1) and (3.4) in the thermodynamic limit, the total grand canonical free energy Ω of the polymer solution within the slit is

$$\Omega = -n_p k_b T A L \omega, \quad (3.8)$$

with

$$\omega = \frac{1}{L}\int_0^L dz \frac{\hat{\mathcal{Z}}_i(z)}{\hat{\mathcal{Z}}_b}. \quad (3.9)$$

Taking into account Eqs. (3.4) and (3.8) we can write for unit surface area $A=1$:

$$\frac{\Omega}{n_p k_B T} = f_b L + f_{s_1} + f_{s_2} + \delta f, \quad (3.10)$$

with the reduced bulk free energy per unit volume $f_b=-1$ and the reduced surface free energy per unit area

$$f_{s_i} = \int_{V_{HS_i}} dz \left(1 - \frac{\hat{\mathcal{Z}}_{HS_i}(z)}{\hat{\mathcal{Z}}_b}\right). \quad (3.11)$$

Further for the sake of convenience we can introduce $\mathcal{X}$, the total system susceptibility in the form

$$\mathcal{X} = \frac{1}{V}\int_V \int_V d^d x d^d x' \langle \vec{\phi}_1(\mathbf{x})\vec{\phi}_1(\mathbf{x}')\rangle. \quad (3.12)$$

This definition is consistent with the bulk susceptibility for the unbounded space given as $\mathcal{X}_b = 1/m^2$ to all orders of renormalized perturbation theory (e.g., [16]). $\hat{\mathcal{Z}}_b$ being the inverse Laplace transform of $\mathcal{X}_b$ and $\hat{\mathcal{Z}}_b = 1$ to all orders as well. Accordingly to Eqs. (2.6) and (3.12) we can rewrite Eq. (3.4) in the form

$$\delta f = \mathcal{IL}_{\mu^2\to R_x^2/2}\{L(\mathcal{X}_b - \mathcal{X}_\parallel) - \Upsilon_1 - \Upsilon_2\}, \quad (3.13)$$

where $\mathcal{X}_\parallel$ denotes the total susceptibility for the slit geometry and Υ_i with $i=1,2$ give two HS contributions such that $f_{s_i} = \mathcal{IL}_{\mu^2\to R_x^2/2}\{\Upsilon_i\}$, (see Appendix B).

IV. CORRELATION FUNCTIONS AND RENORMALIZATION CONDITIONS

Correlation functions, which involve N' fields $\phi(\mathbf{x}_i)$ at distinct points $\mathbf{x}_i (1\le i\le N')$ in bulk, M_1 fields $\phi_1(\mathbf{r}_{j_1}, z=0)$

$\equiv \phi_{s_1}(\mathbf{r}_{j_1})$ at distinct points on the wall $z=0$ and M_2 fields $\phi_2(\mathbf{r}_{j_2}, z=L) \equiv \phi_{s_2}(\mathbf{r}_{j_2})$ at distinct points on the wall $z=L$, and I insertion of the bulk operator $\frac{1}{2}\phi^2(\mathbf{X}_k)$ at points $\mathbf{X}_k$ with $1 \le k \le I$, I_1 insertions of the surface operator $\frac{1}{2}\phi^2_{s_1}(\mathbf{R}_{l_1})$ at points $\mathbf{R}_{l_1}$ with $1 \le l_1 \le I_1$, and I_2 insertions of the surface operator $\frac{1}{2}\phi^2_{s_2}(\mathbf{R}_{l_2})$ at points $\mathbf{R}_{l_2}$ with $1 \le l_2 \le I_2$, have the form [17,25]

$$G^{(N',M_1,M_2,I,I_1,I_2)}(\{\mathbf{x}_i\},\{\mathbf{r}_{j_1}\},\{\mathbf{r}_{j_2}\},\{\mathbf{X}_k\},\{\mathbf{R}_{l_1}\},\{\mathbf{R}_{l_2}\}) = \left\langle \prod_{i=1}^{N'} \phi(\mathbf{x}_i) \prod_{j_1=1}^{M_1} \phi_{s_1}(\mathbf{r}_{j_1}) \prod_{j_2=1}^{M_2} \phi_{s_2}(\mathbf{r}_{j_2}) \prod_{k=1}^{I} \frac{1}{2}\phi^2(\mathbf{X}_k) \prod_{l_1=1}^{I_1} \frac{1}{2}\phi^2_{s_1}(\mathbf{R}_{l_1}) \prod_{l_2=1}^{I_2} \frac{1}{2}\phi^2_{s_2}(\mathbf{R}_{l_2}) \right\rangle. \tag{4.1}$$

Here, the symbol $\langle \ldots \rangle$ denotes averaging with Hamiltonian (2.2). The free propagator of model (2.2) in the mixed $\mathbf{p},z$ representation has form (2.9), as was mentioned above.

Taking into account that surface fields $\phi_{s_i}(\mathbf{r}_{j_i})$ and surface operators $\frac{1}{2}\phi^2_{s_i}(\mathbf{R}_i)$ with $i=1,2$ scale with scaling dimensions that are different from those of their bulk analogs $\phi(\mathbf{x}_j)$ and $\frac{1}{2}\phi^2(\mathbf{X}_j)$ (see [17]), the renormalized correlation functions involving N' bulk fields and M_1 surface fields on the wall $z=0$ and M_2 surface fields on the wall $z=L$, I bulk operators, I_1 and I_2 surface operators can be written as

$$\begin{aligned} G_R^{(N',M_1M_2,I,I_1,I_2)}(;\mu,v,c_1,c_2,L) &= Z_\phi^{-(N'+M_1+M_2)/2} Z_1^{-M_1/2} Z_2^{-M_2/2} Z_{\phi^2}^{I} Z_{\phi^2_{s_1}}^{I_1} Z_{\phi^2_{s_2}}^{I_2} \\ &\times G^{(N',M_1,M_2,I,I_1,I_2)}(;\mu_0,v_0,c_{1_0},c_{2_0},L), \end{aligned} \tag{4.2}$$

where Z_ϕ, Z_1, Z_2 and Z_{ϕ^2}, $Z_{\phi^2_{s_1}}$, $Z_{\phi^2_{s_2}}$ are correspondent UV-finite (for $d<4$) renormalization factors. The typical bulk and surface short-distance singularities of the correlation functions $G^{(N',M_1,M_2)}$ can be removed via a mass shift $\mu_0^2 = \mu^2 + \delta\mu^2$ and surface-enhancement shifts $c_{i_0} = c_i + \delta c_i$, respectively [17]. The renormalizations of the mass μ, the coupling constant v, and the renormalization factor Z_ϕ are defined by standard normalization conditions of the infinite-volume theory [16,28–31]. In order to adsorb uv singularities located in the vicinity of the surfaces, the surface-enhancement shifts δc_i are required. In connection with this the new normalization conditions should be introduced. It is obvious that in the limit $L \to \infty$ we should have

$$\lim_{L\to\infty}[\tilde{G}_R^{(0,2,0)}(\mathbf{p};\mu,v,c_1,c_2,L)|_{p=0}] = \frac{1}{\mu + c_1},$$

$$\lim_{L\to\infty}[\tilde{G}_R^{(0,0,2)}(\mathbf{p};\mu,v,c_1,c_2,L)|_{p=0}] = \frac{1}{\mu + c_2}. \tag{4.3}$$

For the renormalization factors Z_i, $Z_{\phi^2_{s_i}}$, where $i=1,2$ we obtain, respectively,

$$\lim_{L\to\infty}\left[\frac{\partial}{\partial p^2}\tilde{G}_R^{(0,2,0)}(\mathbf{p};\mu,v,c_1,c_2,L)|_{p=0}\right] = -\frac{1}{2\mu(\mu+c_1)^2},$$

$$\lim_{L\to\infty}\left[\frac{\partial}{\partial p^2}\tilde{G}_R^{(0,0,2)}(\mathbf{p};\mu,v,c_1,c_2,L)|_{p=0}\right] = -\frac{1}{2\mu(\mu+c_2)^2}, \tag{4.4}$$

and

$$\lim_{L\to\infty}[\tilde{G}_R^{(0,2,0;0,1,0)}(\mathbf{p},\mathbf{P};\mu,v,c_1,c_2,L)|_{p,P=0}] = \frac{1}{(\mu+c_1)^2},$$

$$\lim_{L\to\infty}[\tilde{G}_R^{(0,0,2;0,0,1)}(\mathbf{p},\mathbf{P};\mu,v,c_1,c_2,L)|_{p,P=0}] = \frac{1}{(\mu+c_2)^2}. \tag{4.5}$$

In the limit $L\to\infty$ all these conditions yield exactly the same shifts δc_i and renormalization factors as in the semi-infinite case. It is intuitively clear that in the case of two inert walls or mixed walls situated at big but finite distance L with $L \gtrsim R_g$ such that the chain is still not deformed too much from its original size in bulk, the shift of $c_0^{sp} \to c^{sp}$ may depend on the presence of the other surface and hence on the size of the slit. So, in the case of $L \gtrsim R_g$ (or $\mu L \gtrsim 1$) from Eqs. (2.9) and (4.3) we obtain conditions

$$\begin{aligned} &\lim_{L\mu\gtrsim 1}[\tilde{G}_R^{(0,2,0)}(\mathbf{p};\mu,v,c_1,c_2,L)|_{p=0}] \\ &\quad = \frac{1}{\mu+c_1}\left(1 + \frac{2\mu}{\mu+c_1}\frac{\mu-c_2}{\mu+c_2}e^{-2\mu L} + \mathcal{O}(e^{-4\mu L})\right), \\ &\lim_{L\mu\gtrsim 1}[\tilde{G}_R^{(0,0,2)}(\mathbf{p};\mu,v,c_1,c_2,L)|_{p=0}] \\ &\quad = \frac{1}{\mu+c_2}\left(1 + \frac{2\mu}{\mu+c_2}\frac{\mu-c_1}{\mu+c_1}e^{-2\mu L} + \mathcal{O}(e^{-4\mu L})\right). \end{aligned} \tag{4.6}$$

The above-mentioned conditions (4.6) give one-loop order corrections to the respective surface-enhancement shifts δc_i of semi-infinite theory in the case of large but finite wall separation L. In accordance with this, for the case of mixed walls we obtain

$$\delta c_1^{S-O} = \delta c_1 + \Delta^{(S-O)}, \tag{4.7}$$

with corrections of order $\mathcal{O}(e^{-2\mu L})$

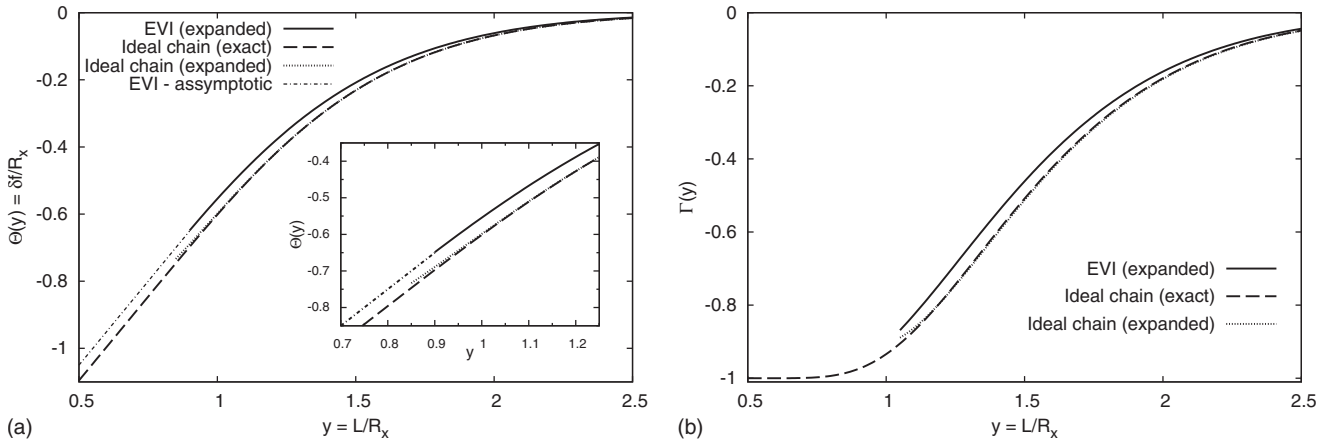

FIG. 1. The functions $\Theta(y)$ and $\Gamma(y)$ for two repulsive walls.

$$\Delta^{(S-O)} = \frac{\mu}{4}\left(\frac{1}{\mu L} + C_E + \ln 8 - 3 + \ln \mu L - e^{4\mu L}\mathrm{Ei}(-4\mu L)\right)e^{-2\mu L}. \tag{4.8}$$

In the case when both walls are inert, the modified surface-enhancement shifts are

$$\delta c_i^{S-S} = \delta c_i + \Delta^{(S-S)}, \tag{4.9}$$

with

$$\Delta^{(S-S)} = -\Delta^{(S-O)} - \mu\left(\ln 2 - \frac{1}{2}\right)e^{-2\mu L}. \tag{4.10}$$

The above-mentioned corrections δc_i are UV singular for $d=3$ dimensions. They provide the singular parts of the counterterms that cancel the UV singularities of the correspondent correlation functions by analogy as it took place for semi-infinite systems (see [17]). The above-mentioned corrections $\Delta^{(S-O)}$ and $\Delta^{(S-S)}$ are finite in $d \leq 4$ dimensions.

V. RESULTS FOR GAUSSIAN CHAINS

Let us consider at the beginning the case of ideal polymer chains ($v_0=0$). As mentioned above it corresponds to the situation of a polymer chain under Θ-solvent conditions.

For general case of arbitrary c_1 and c_2 on the confining walls, we obtain for the reduced free energy of interaction:

$$\delta f = -\mathcal{IL}_{\mu^2 \to R_x^2/2}\left\{\frac{1}{\mu^3}[(\mu+c_1)(\mu+c_2)e^{\mu L} - (\mu-c_1)(\mu-c_2)e^{-\mu L}]^{-1}\{4c_1c_2 - [\mu(c_1+c_2)+2c_1c_2]e^{\mu L} + [\mu(c_1+c_2)-2c_1c_2]e^{-\mu L}\} + \frac{1}{\mu^3}\left(\frac{c_1}{\mu+c_1} + \frac{c_2}{\mu+c_2}\right)\right\}. \tag{5.1}$$

First, consider the case of Dirichlet-Dirichlet (D-D) boundary conditions (2.3) on the confining surfaces. Taking the limits $c_1/m \to \infty, c_2/m \to \infty$ yields

$$\Theta^{D,D}(y) = -4y\mathcal{IL}_{\tau \to (2y^2)^{-1}}\left(\frac{1}{\tau^{3/2}}\frac{1}{1+e^{\sqrt{\tau}}}\right), \tag{5.2}$$

where $\tau = \mu^2 L^2$ and $y = L/R_x$. The result indicates that if both c_1 and c_2 are positive, the depletion interaction potential is negative and hence the walls attract each other due to the depletion zones near repulsive walls. The inverse Laplace transform can only be performed numerically (the plot is shown in Fig. 1) or may be expanded for asymptotic values of $\sqrt{\tau}$. The obtained results for ideal polymer chains in slit of two repulsive walls are in agreement with previous theoretical results obtained in Ref. [14]. However, it should be mentioned that on plotting these functions the authors of [14] used a rescaled variable $\sqrt{2}R_x$, which was not mentioned there.

Now we proceed to the case of two inert walls, which corresponds to Neumann-Neumann (N-N) boundary conditions (2.4). For the free energy of interaction we obtain

$$\Theta^{N,N}(y) = 0. \tag{5.3}$$

It corresponds to the fact that ideal chains do not loose free energy inside the slit in comparison with free chains in unrestricted space. The entropy loss is fully regained by surface interactions provided by two walls.

Taking the limits $\frac{c_1}{m} \to \infty, \frac{c_2}{m} \to 0$ in accordance with Eq. (2.5) [Dirichlet-Neumann (D-N) boundary conditions] from Eq. (5.1) we obtain

$$\Theta^{D,N}(y) = -2y\mathcal{IL}_{\tau \to (2y^2)^{-1}}\left(\frac{1}{\tau^{3/2}}\frac{1}{1+e^{2\sqrt{\tau}}}\right). \tag{5.4}$$

This result can only be evaluated numerically and is plotted in Fig. 2. From comparison Eqs. (5.2) and (5.4) it is easily to see that

$$\Theta^{D,D}(2y) = 2\Theta^{D,N}(y). \tag{5.5}$$

The obtained result is intuitively clear, because the depletion zone is formed only near the lower wall, i.e., near the wall with Dirichlet bc. The upper wall with Neumann bc does not contribute at all to the induced depletion interaction. Let us consider different asymptotic regions of y.

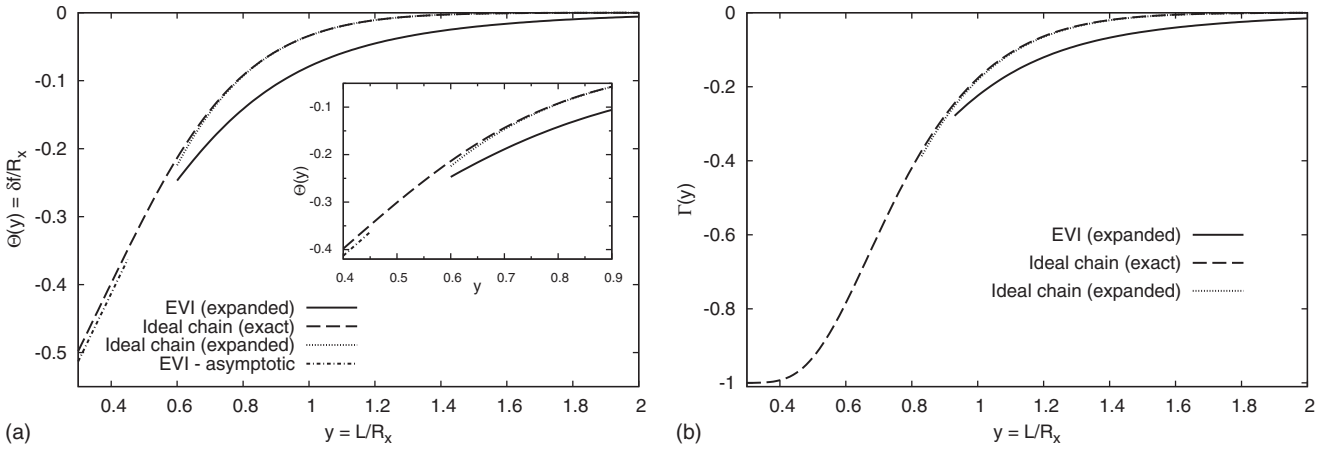

FIG. 2. The functions $\Theta(y)$ and $\Gamma(y)$ for one repulsive and one inert wall with and without excluded volume interactions (EVI).

A. Wide slits ($y \gg 1$)

In the case $\mu L \gg 1$ from Eq. (5.2) we obtain for two repulsive walls:

$$\Theta^{D,D}(y) \approx 4y\left[\operatorname{erfc}\left(\frac{y}{\sqrt{2}}\right) - \frac{1}{y}\sqrt{\frac{2}{\pi}}\exp\left(-\frac{y^2}{2}\right)\right] - 8y\left[\operatorname{erfc}(\sqrt{2}y) - \frac{1}{y\sqrt{2\pi}}\exp(-2y^2)\right]. \quad (5.6)$$

The force [Eq. (3.7)] becomes

$$\Gamma^{D,D}(y) \approx -4\operatorname{erfc}\left(\frac{y}{\sqrt{2}}\right) + 8\operatorname{erfc}(\sqrt{2}y). \quad (5.7)$$

And for one repulsive and one inert wall we have

$$\Theta^{D,N}(y) \approx 4y\operatorname{erfc}(\sqrt{2}y) - \frac{4}{\sqrt{2\pi}}\exp(-2y^2), \quad (5.8)$$

which implies

$$\Gamma^{D,N}(y) \approx -4\operatorname{erfc}(\sqrt{2}y). \quad (5.9)$$

These approximating functions are presented in Figs. 1 and 2, respectively.

B. Narrow slits ($y \ll 1$)

In the case of narrow slit $\mu L \ll 1$ the asymptotic solution for Eq. (5.2) reads as

$$\Theta^{D,D}(y) \approx -\frac{4}{\sqrt{2\pi}} + y, \quad (5.10)$$

and the force simply becomes $\Gamma^{D,D}(y) \approx -1$.

For the depletion interaction potential [Eq. (5.4)] we get

$$\Theta^{D,N}(y) \approx -\frac{2}{\sqrt{2\pi}} + y. \quad (5.11)$$

For the force we have again $\Gamma^{D,N}(y) \approx -1$.

These results can be understood phenomenologically. In our units the quantities Θ and Γ are normalized to the overall polymer density n_p. So, the above results simply indicate that the force is entirely induced by free chains surrounding the slit or, in other words, by the full bulk osmotic pressure from the outside of the slit. No chain has remained in the slit. It is reasonable in the case of repulsive walls in the limit of narrow slits. Unfortunately, the narrow slit regime is beyond the validity of our approach in the presence of EVI as mentioned above. But the above-mentioned arguments can be used in order to obtain the leading contributions to the depletion ef-

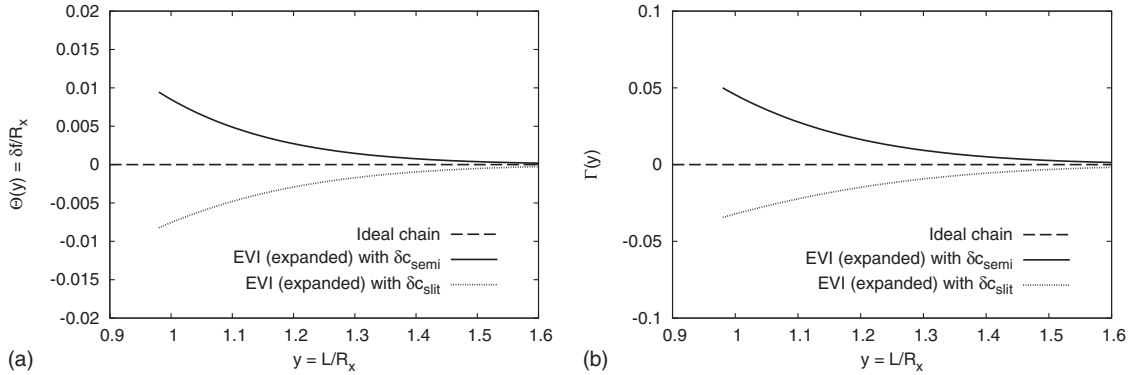

FIG. 3. The functions $\Theta(y)$ and $\Gamma(y)$ for two inert walls with and without EVI. Here we introduced notations: $\delta c_{semi} = \delta c_i$ and $\delta c_i^{S-S} = \delta c_{slit}$, with $i = 1, 2$.

fect as $y \to 0$. We can state that in the case of very narrow slits the chains would pay a very high entropy to stay in the slit or even enter it. It is due to the fact that the phase space containing all possible conformations is essentially reduced by the squeezing confinement to the size $\frac{d-1}{d}$ times its original size (for an unconfined chain). Therefore, the ratio of partition function of polymer chain in the slit and the free chain partition function vanishes strongly as $y \to 0$, which implies directly the function ω in Eq. (3.9). Setting $\omega=0$ and using only the corresponding surface contributions and the bulk contribution ($f_b=-1$) in Eq. (3.10) must lead to the same asymptotic limits in the narrow slit regime. The advantage of this procedure is that no expansion is necessary and it should be equally valid in the EVI regime.

In Figs. 1–3 the depletion interaction potential $\Theta(y)$ and depletion force $\Gamma(y)$ are plotted for all boundary conditions. As expected, the results for mixed walls are located in between the results of two inert walls and those of two repulsive walls.

VI. RESULTS FOR GOOD SOLVENT

In good solvent the EVI between monomers play a crucial role so that polymer coils occupy the bigger volume and are less compact than in the case of ideal polymer chains. The influence of the EVI on the depletion functions can be obtained within the framework of the massive field theory approach in fixed dimensions $d=3$ up to one-loop order approximation of the two-point correlation functions $G^{(2,0,0)}$ restricted to the slit geometry [Eq. (2.2)]. The bare total susceptibility $\mathcal{X}_{\parallel}^{bare}$ [see Eq. (3.13)] for the slit geometry in accordance with Eqs. (3.9), (3.12), and (4.1) is

$$\mathcal{X}_{\parallel}^{bare}(\mu_0,v_0,c_{1_0},c_{2_0},L)=\frac{1}{L}\int_0^L\int_0^L dzdz'\Bigg\{\tilde{G}_{\parallel}(\mathbf{p}=0,z,z';\mu_0,c_{i_0},L) - \frac{n+2}{6}v_0\int_0^L dz''\int_{\mathbf{q}}\tilde{G}_{\parallel}(\mathbf{p}=0,z,z'';\mu_0,c_{i_0},L)\tilde{G}_{\parallel}(\mathbf{q},z'',z'';\mu_0,c_{i_0},L)\tilde{G}_{\parallel}(\mathbf{p}=0,z'',z';\mu_0,c_{i_0},L)\Bigg\}. \tag{6.1}$$

The two HS contributions denoted by Υ_i [see Eq. (3.13)] can be obtained in accordance with Eq. (3.11) similarly to Eq. (6.1) with the propagators of semi-infinite system. Some details of the calculation of these quantities for zero-loop and one-loop orders for different surface critical points of interest (ordinary, special) are presented in Appendix B. In order to make the theory UV finite in renormalization-group (RG) sense in $3 \le d < 4$ dimensions, we perform the standard mass renormalization, the coupling constant renormalization, and additional surface-enhancement constants renormalization.

A. Two repulsive walls

Let us first consider the case of D-D boundary conditions (2.3) on each of two surfaces. Each surface term ($f_{s_i}, i=1,2$) contributes

$$f_s^D=\sqrt{\frac{2}{\pi}}\left(1-\frac{\ln\frac{9}{8}}{4}\right)R_x. \tag{6.2}$$

It should be mentioned that in the limit $c_i \to \infty$ (where $i=1,2$) surface-enhancement constants renormalization reduces to an additive renormalization by analogy as it took place for the case of semi-infinite geometry [17]. After performing the standard mass and the coupling constant renormalization and additive renormalization at zero momentum, the correspondent function $\mathcal{X}_{\parallel ren}^{D,D}$ can be obtained. In order to be concise, we do not present here the complicated form for $\mathcal{X}_{\parallel ren}^{D,D}$ and just discuss the limiting cases of wide and narrow slit regimes.

1. Wide slits ($y \gtrsim 1$)

The massive field-theory approach at fixed dimensions $d=3$ gives a rather simpler result in one-loop order than the results obtained in [14] with the help of dimensionally regularized field theory with minimal subtraction of poles in ε expansion. It should be mentioned that in [14] the wide slit approximation was carried out as well up to the first nontrivial order [apparently $\mathcal{O}(e^{-\mu L})$]. Therefore, we performed calculations up to the next-order term $\sim \mathcal{O}(e^{-2\mu L})$. The renormalized total susceptibility for the slit geometry up to one-loop order in $d=3$ for polymer case $n \to 0$ in the wide slits regime $\mu L \gg 1$ is

$$\mathcal{X}_{\parallel ren}^{D,D}L \approx \frac{L}{\mu^2}-\frac{1}{\mu^3}\left(2-\frac{\ln\frac{9}{8}}{2}\right)+\frac{e^{-\mu L}}{\mu^3}\left(4-\ln\frac{3}{2}\right)-\frac{e^{-2\mu L}}{\mu^3} \times\Bigg\{\frac{9-C_E-2\ln\frac{3}{2}}{2}-\frac{3}{2\mu L}-\frac{\ln(\mu L)}{2}+e^{\mu L}\mathrm{Ei}(-\mu L) - e^{3\mu L}\mathrm{Ei}(-3\mu L)+\frac{e^{4\mu L}}{2}\mathrm{Ei}(-4\mu L)\Bigg\}. \tag{6.3}$$

The exponential integral functions, denoted by $\mathrm{Ei}(x)$, can be expanded for large negative arguments as well in accordance with (see, e.g., [32]): $e^x\mathrm{Ei}(-x)=-1/x+\mathcal{O}(1/x^2)$. Thus, for the depletion interaction potential we obtain

$$\Theta(y) \approx \left(4 - \ln\frac{3}{2}\right)\left[y\ \mathrm{erfc}\left(\frac{y}{\sqrt{2}}\right) - \sqrt{\frac{2}{\pi}}\exp\left(\frac{y^2}{2}\right)\right] - \frac{55}{48y}\mathrm{erfc}(\sqrt{2}y) - \left(\frac{163}{24} - \ln\frac{3}{2} - \frac{C_E}{2}\right)\left[2y\ \mathrm{erfc}(\sqrt{2}y) - \sqrt{\frac{2}{\pi}}\exp(-2y^2)\right] - \frac{y}{4}\mathcal{IL}_{\tau\to 1/2y^2}\left(\frac{\ln\tau}{\tau^{3/2}}e^{-2\sqrt{\tau}}\right). \quad (6.4)$$

The comparison of the obtained results to ideal chain results in the wide slit regime (see Fig. 1) shows that the EVI reduces the depletion effects for two repulsive walls.

2. Narrow slits ($y \ll 1$)

Following the simple argument obtained from the discussion of the exactly solvable ideal chain model, the entire slit contribution ω [Eq. (3.9)] to the reduced free energy of interaction δf in Eq. (3.10) is simply set to zero, and the depletion effect is only calculated from bulk and surface contributions. In this limit the depletion potential becomes

$$\Theta(y) \approx y - \frac{2\sqrt{2}}{\sqrt{\pi}}\left(1 - \frac{\ln\frac{9}{8}}{4}\right), \quad (6.5)$$

and the force again is unity. In Fig. 1 one can follow how the two regimes come to match in the crossover regime $y \approx 1$. The lowest-order expansion in the case of wide slits is unable to show this matching. With these two approximations we are in the position to present a rather complete picture of the problem in comparison with the approach given in [14].

B. One repulsive–One inert wall

This case has not been studied so far in any approach. Since we are now dealing with an inert wall, the surface-enhancement constant shift should be taken into account. Again, the full result for the renormalized total susceptibility of system within the slit $\mathcal{X}_{\|ren}$ has complicated form and we here focused our discussion on the limiting cases of wide and narrow slits only.

The surface contribution for the repulsive wall coincides with Eq. (6.2) and for the inert wall we have

$$f_s^N = \frac{2\ln 2 - 1}{8}\sqrt{\frac{2}{\pi}}R_x. \quad (6.6)$$

1. Wide slits ($y \gtrsim 1$)

For the total susceptibility up to $\mathcal{O}(\mathrm{e}^{-2\mu L})$ order we obtain

$$\mathcal{X}_{\|ren}^{OS}L \approx \frac{L}{\mu^2} - \frac{1}{\mu^3}\left(1 + \frac{2\ln\frac{4}{3} - \frac{1}{2}}{4}\right) + \frac{e^{-\mu L}}{\mu^3}\left(\frac{2\ln 4 - \ln 3 - 1}{2}\right) + \frac{e^{-2\mu L}}{\mu^3}\left\{\frac{31 - 2C_E}{8} - \frac{\ln 3}{2} - \frac{7\ln 2}{4} - \frac{3}{4\mu L} - \frac{\ln(\mu L)}{4} + \frac{e^{\mu L}}{2}\mathrm{Ei}(-\mu L) + \frac{e^{4\mu L}}{4}\mathrm{Ei}(-4\mu L) - \frac{e^{3\mu L}}{2}\mathrm{Ei}(-3\mu L)\right\}. \quad (6.7)$$

In comparison with the result for ideal chains [Eq. (5.4)], where the lowest-order term contributing to the total susceptibility in the wide slit limit is of order $\mathcal{O}(e^{-2\mu L})$, now the additional term of order $\mathcal{O}(e^{-\mu L})$ appears.

In this case the depletion interaction potential becomes

$$\Theta(y) \approx \frac{1}{2}\left(\ln\frac{16}{3} - 1\right)\left[y\ \mathrm{erfc}\left(\frac{y}{\sqrt{2}}\right) - \sqrt{\frac{2}{\pi}}\exp\left(-\frac{y^2}{2}\right)\right] + \frac{55}{96y}\mathrm{erfc}(\sqrt{2}y) + \frac{1}{4}\left(\frac{229}{12} - C_E - \ln 1152\right)\times\left[2y\ \mathrm{erfc}(\sqrt{2}y) - \sqrt{\frac{2}{\pi}}\exp(-2y^2)\right] + \frac{y}{8}\mathcal{IL}_{\tau\to 1/2y^2}\left(\frac{\ln\tau}{\tau^{3/2}}e^{-2\sqrt{\tau}}\right). \quad (6.8)$$

Figure 2 presents the depletion interaction potential $\Theta(y)$ and the force $\Gamma(y)$. It clearly indicates that in comparison with ideal chains the depletion effect is stronger in the regime of wide slits.

2. Narrow slits ($y \ll 1$)

Following again the thermodynamic argument, ω is set to zero and only bulk and surface contributions are taken into account in Eq. (3.10). One gets

$$\Theta(y) \approx y - \left(1 + \frac{2\ln\frac{4}{3} - \frac{1}{2}}{4}\right)\sqrt{\frac{2}{\pi}}, \quad (6.9)$$

which is also slightly below the depletion potential in comparison with the case of ideal chains (see Fig. 2). The depletion force is unity.

Both approximations for wide, as well as for narrow slits suggest the depletion effect to be stronger in the case of excluded volume interactions than for ideal polymer chains (see Fig. 2).

C. Two inert walls

In order to obtain the renormalized total susceptibility for a system confined by two parallel inert walls we have to apply the surface renormalization scheme suggested by [17] for both surfaces at their surface critical point $c_{i_0}^{sp}$. Starting from Eq. (6.1) we obtain for the renormalized total susceptibility:

$$\mathcal{X}_{\|ren}^{SS}L = \frac{L}{\mu^2} - \frac{1}{2\mu^3}\left(\ln 2 - \frac{1}{2} - \ln(1 - e^{-2\mu L})\right). \quad (6.10)$$

The surface contribution has already been presented in Eq. (6.6). Let us consider the asymptotic expansion for wide slits $\mu L \gg 1$. Taking into account the surface [Eq. (6.6)] and bulk contributions, the result for the depletion interaction potential becomes

$$\Theta(y) \approx \frac{1}{\sqrt{2\pi}}e^{-2y^2} - y\ \mathrm{erfc}(\sqrt{2}y). \quad (6.11)$$

This function and its derivative for the force are plotted in Fig. 3.

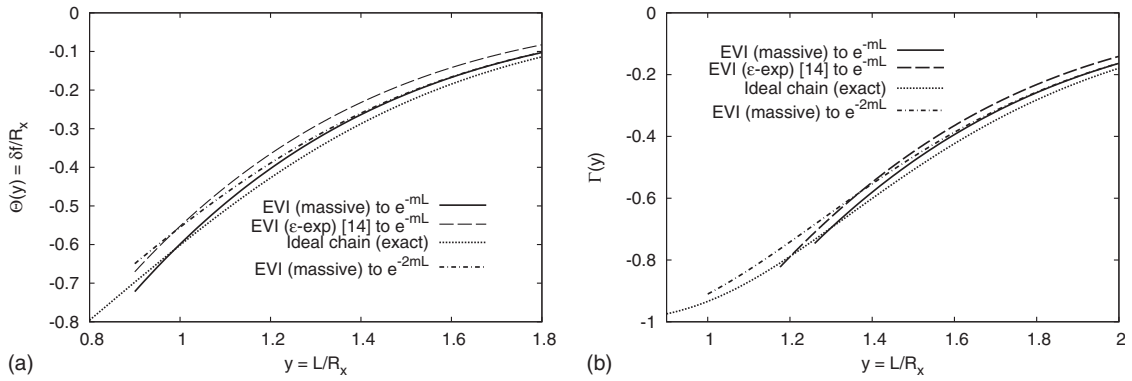

FIG. 4. The functions $\Theta(y)$ and $\Gamma(y)$ for two repulsive walls in comparison to [14].

It is obvious that only the wide slit approximation can be applied here since the usual argument for the narrow slit approximation is no more valid and ω does not necessarily vanish.

Interestingly, the depletion force turns out to be positive and the walls are repelled from each other. It means that polymer chains like to stay in between the slit rather than leave it. Thus, the chains gain enough energy from attractive interactions on the walls, which forces them to exert their loss of entropy (due to the confinement) onto walls instead of leaving the slit.

It is very instructive to have a more general look on the terms appearing in the free energy of interaction. If we now take into account new normalization conditions for surface-enhancement constants for slit geometry [see Eqs. (4.6)–(4.10)], which assume that we have big, but finite wall separation L, the δf can be written as

$$\delta f = 2\mathcal{I}\mathcal{L}_{\mu^2 \to R_x^2/2}\left(\frac{\delta c_i^{S-S} - \delta c_i}{\mu^4}\right) - \mathcal{I}\mathcal{L}_{\mu^2 \to R_x^2/2}\left(\frac{\ln(1-e^{-2\mu L})}{2\mu^3}\right). \tag{6.12}$$

Here δc^{S-S} is the surface-enhancement constant shift for the slit geometry which appears in the case of finite walls separation and δc_i is the surface-enhancement constant shift in the case of infinite walls separation. In the presented approach the same renormalization of critical values c_0^{sp} was used and equally the same shifts to the renormalized values were obtained. So the first term on the rhs just disappeared on the assumption that the surface-enhancement constant shift on one surface is not affected by the presence of the second one.

In fact, this assumption could be doubted and an additional shift through the influence of the second wall (a coupling effect between two walls) may appear. Since the interaction potential itself is purely local, such coupling effect can only be mediated through chain conformations. As a result, the number density of monomers near the walls might differ in comparison with a semi-infinite constraint, and also the shift of the critical point (due to excluded volume interactions) can change. As already proposed in [33] this in turn would require a different renormalization scheme for the surface critical point, where this coupling effect is to be taken into account. The results of calculations for a slightly modified surface renormalization scheme which takes into account the finite surface separation L are introduced at Appendix C and are presented in Fig. 3 as well. It should be mentioned that in accordance with this it will be useful to extend in the future the present calculations up to the next two-loop order approximation of renormalized perturbation theory.

VII. COMPARISON TO PREVIOUS WORK

A. Theoretical approach

As was mentioned in the introduction, a remarkable progress in the investigation of the influence of EVI on the depletion interaction and depletion force between two repulsive walls was achieved by [13,14] via using the dimensionally regularized continuum version of the field theory with minimal subtraction of poles in $\epsilon=4-d$, where d is dimensionality of space. Figure 4 presents the comparison of our results obtained within the framework of massive field theory at fixed dimensions $d=3$ for the case of two repulsive walls and results obtained in [14].

The results obtained within the framework of both analytical methods are in quantitative agreement. But one notes that the reduction in the depletion effect due to excluded volume interactions is weaker within the massive field approach as compared to an ϵ expansion in one-loop order. It should be noted that we extended our results up to the next $e^{-2\mu L}$ order. This allowed us to obtain good matching with approximating results in the narrow slit limit [see Figs. 1 and 2 for $\theta(y)$].

B. Simulations

One of the possibilities to test the reliability of the obtained analytical results is to compare them with the results obtained by Monte Carlo simulations. In this section we compare our results with the results of MC calculations obtained by [19,20] for the single polymer chain trapped inside the slit of two repulsive walls, which corresponds to a canonical ensemble. The canonical free energy can be obtained via the Legendre transform from the grand canonical one in the thermodynamic limit $(N, V \to \infty)$ in the form

$$F(N_l) = \Omega[\mu(N_l)] + \mu(N_l)N_l, \tag{7.1}$$

with Ω from Eq. (3.8).

Thus, the reduced canonical force for the one polymer chain $N_l=1$ can be written as its dimensionless counterpart:

$$\frac{KL}{k_bT} = \frac{1}{\omega}\frac{d}{dL}(L\omega). \tag{7.2}$$

It should be mentioned that both Monte Carlo algorithms (see [19,20]) differ very much from each other in the range of analyzed slit widths and chain lengths of the simulated polymers. In [19] an off-lattice bead and spring model for the self-avoiding polymer chain in $d=3$ dimensions trapped between two parallel repulsive walls at distance D has been studied by Monte Carlo methods using chain lengths up to $N \leq 512$ (number of monomers in the chain) and distances D from 4 to 32 (in units of the maximum spring extension). It was stated that the total force K exerted on the walls is repulsive and diverges for the case of narrow slit as

$$\frac{KL}{k_bT} \sim \left(\frac{L}{R_g}\right)^{-1/\nu}, \tag{7.3}$$

where R_g is the radius of gyration of the polymer chain in unrestricted geometry.

In Ref. [20] the lattice Monte Carlo algorithm on a regular cubic lattice in three dimensions, with D lattice units in z direction and impenetrable boundaries was applied. The other directions obeyed periodic boundary conditions. The proposed MC simulations [20] are based on the analytical result obtained by [13] for the scaling behavior of partition function for a chain confined to the slit geometry of width D:

$$Z_N(D) \propto (\mu_\infty + aD^{-1/\nu})^{-N} N^{\gamma_2-1} D^{(\gamma_2-\gamma_3)/\nu}, \tag{7.4}$$

for $N,D \to \infty$, but $D \ll N^\nu$, where μ_∞ is the critical fugacity per monomer and γ_d is the universal exponent [see Eq. (2.1)] dependent on the space dimension d and the parameter a is a universal amplitude. The critical fugacity means the averaged inverse number of possible steps at each site. In [20] universal amplitudes and exponents for the partition function of the chain trapped in the slit with respect to that of a free chain have been obtained through analyzing the statistics for different D and number of chain monomers up to $N \leq 80\,000$. Also both cases of ideal chains [modeled as a simple random walk (RW)] and chains with excluded volume interactions [modeled via self-avoiding walks (SAWs)] have been studied. In the case of an ordinary random walk on a regular cubic lattice in three dimensions one has obviously $\mu_\infty = \frac{1}{6}$ and $\gamma_{d=3}=1$. In the case of SAW on such a lattice it is clear that at least $\mu_\infty \geq \frac{1}{5}$. From Eq. (7.4) one may obtain the force exerted onto the walls in units of k_BT as

$$\tilde{K} = k_BT\frac{d}{dD}\ln[Z_N(D)]. \tag{7.5}$$

In the limit ($D \ll N^\nu$, $N,D \to \infty$) $\tilde{K}$ becomes

$$\tilde{K} = k_BT\left(\frac{Na}{\nu\mu_\infty}D^{-1-1/\nu}\right). \tag{7.6}$$

One should note that all functions here are in terms of dimensionless length scales, the number of lattice sites (D and N). In order to compare with our results, it must be translated into terms of L and R_g. Apparently $L=uD$, with u denoting the lattice spacing, and the reduced dimensionless force reads as

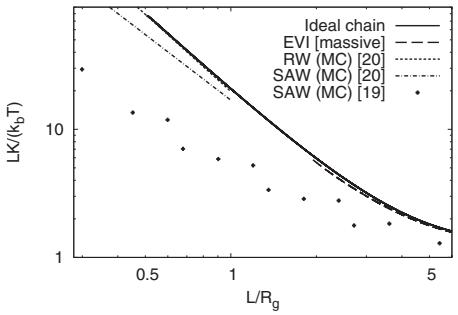

FIG. 5. Comparison of our theoretical results with Monte Carlo simulations for a *trapped* chain between two repulsive walls. The plots Ideal chain (exact) and EVI (wide slit) represent the results of our calculations. RW (MC) and the first SAW (MC) are due to the estimated asymptotic behavior in the narrow slit limit by [20] for random walks and self avoiding walks. The second SAW (MC) are the results obtained by [19].

$$k = \frac{\tilde{K}D}{k_BT} = \frac{a}{\nu_3\mu_\infty}\left(\frac{6}{\chi_d^2}\right)^{1/2\nu_3}\left(\frac{L}{R_g}\right)^{-1/\nu_3}, \tag{7.7}$$

where we take into account the general relation (e.g., [21]):

$$R_g^2 = \chi_3^2\frac{b^2N^{2\nu_3}}{6} \tag{7.8}$$

in $d=3$ dimensions. Parameter b denotes the (effective) segment length of the polymer model under consideration. In the case of RW and SAW on the cubic lattice one has simply $b=u$ because the segment length in these models is naturally provided by the lattice parameter u. In [20] the universal amplitude a for the case of ideal chains was found as $a \approx 0.2741$, which is very close to the exact value, computed analytically in [13], of $a=\pi^2/36$. Taking into account that for the ideal chain $\nu=0.5$, $\chi_d=1$, and $\mu_\infty=\frac{1}{6}$ the force becomes

$$k_{id} = 2\pi^2\left(\frac{L}{R_g}\right)^{-2}. \tag{7.9}$$

In Fig. 5 this asymptotic behavior for narrow slits is clearly recovered by our results for ideal chains, where the narrow slit limit is valid. By contrast, for a SAW in Ref. [20] the value $a \approx 0.448$ was suggested. Taking into account the values for $\nu \approx 0.588$, $\chi_3 \approx 0.958$ [21], and $\mu_\infty \approx 0.2135$ the reduced force can be written as

$$k_{saw} \approx 16.95\left(\frac{L}{R_g}\right)^{-1.7}. \tag{7.10}$$

Result (7.10) is presented in Fig. 5 in its regime of validity and compared to our theoretical results for a trapped chain with EVI, which are valid for the wide slit regime. As it easily can be seen from Fig. 5, result (7.10) corresponds very well to our predictions in the wide slit limit. Also, in Fig. 5 the results obtained by the authors of Ref. [19] are plotted and one notes a qualitative agreement with our predictions.

One of the possible reasons for remaining deviations with the results of Ref. [19] is that the chain in the MC simulation is too short in order to compare with the results of the field-theoretical RG group approach. It should be noted that at the moment no simulations concerning two inert walls or one inert–one repulsive wall exist.

C. Experiment

In Ref. [5] an experimental study of the depletion effect between a spherical colloidal particle immersed in the dilute solution of nonionic linear polymer chains and the wall of the container through total internal reflection microscopy was analyzed. Using the Derjaguin [7] approximation we could compare our theoretical results with experimental data in the case when the radius of the spherical colloid particle R is much larger than the radius of gyration R_g and the closest distance a between the particle and the surface. The deviation of the experimental setup from the presented theoretical approach is connected with the fact that the *second* wall is not plane but curved. Summing up, the depletion potential per volume unit for the case of two plane surfaces in the margins of the curved volume allows us to estimate the depletion effects in the case of a sphere and a wall. In the experiment by [5] the radius of gyration was measured as $R_g=0.101$ μm and the colloidal particle was reported to have the radius $R=1.5$ μm. A straightforward application of the Derjaguin [7] approximation yields

$$\frac{\phi_{depl}(a)}{n_p k_b T} = 2\pi R_x^2 \int_{a/R_x}^{(a+R)/R_x} dy(R + a - R_x y)\Theta(y), \tag{7.11}$$

with a as the minimal distance between the sphere and the wall. Since in the range of y the last two terms in the parenthesis are much smaller in comparison with the first one, we can assume that

$$\frac{\phi_{depl}(a)}{n_p k_b T} \approx 2\pi R R_x^2 \int_{a/R_x}^{\infty} dy\Theta(y). \tag{7.12}$$

The experimental data in comparison with our theoretical prediction are plotted in Fig. 6. It should be mentioned that our results obtained within the framework of the massive field theory approach are situated slightly closer to the experimental data than previous theoretical results obtained within the framework of the dimensionally regularized continuum version of the field theory with minimal subtraction of poles in $\epsilon=4-d$ [14]. Unfortunately, this shift is not enough in order to obtain quantitative agreement with the experimental data. But the obtained theoretical curves in Fig. 6 are in qualitative agreement with the experimental data. The quantitative discrepancy can be removed if we use the radius of gyration as adjusting parameter by analogy as it was done in [14]. On the other hand, this indicates the importance of further theoretical investigations of the depletion interaction potential and the depletion force in the crossover region from wide to narrow slit.

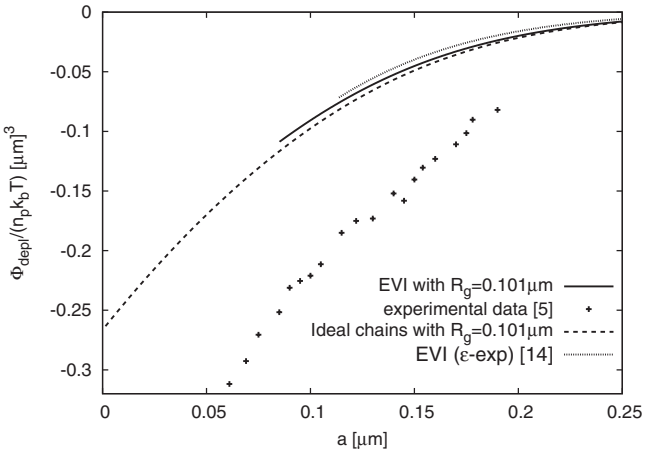

FIG. 6. Comparison of approximated theoretical results with experimental observation due to [5].

VIII. CONCLUSIONS

Using the massive field theory approach directly at fixed dimensions $d=3$ we calculated the depletion interaction potential and the depletion force between two repulsive, two inert, and one repulsive and one inert walls confining the dilute solution of long flexible polymer chains. The obtained calculations for all cases of polymer-surface interactions were performed for the ideal chain and the real polymer chain with EVI in the wide slit regime. Besides, we used some assumptions which allowed us to estimate the depletion interaction potential in the region of narrow slit. Our results have been obtained up to the next $e^{-2\mu L}$ order in comparison with the results of ϵ expansion [14]. Our investigations include the modification of renormalization scheme for the case of two inert walls (or mixed walls) situated on big but finite distance L with $L \gtrsim R_g$ such that the polymer chain is still not deformed too much from its original size in the bulk. In this respect it will be useful to extend in the future the present calculations up to the next two-loop order of renormalized perturbation theory. The obtained results indicate that the reduction in the depletion effect due to EVI is weaker within the massive field theory approach as compared to the dimensionally regularized continuum version of the field theory with minimal subtraction of poles in $\epsilon=4-d$ [14]. We found very good agreement with Monte Carlo simulation data [19,20] for the case of two repulsive walls. Taking into account the Derjaguin approximation we obtained good qualitative agreement with the experimental data [5] for the depletion potential between the spherical colloidal particle of big radius and repulsive wall. From the comparison of obtained theoretical results and experimental data we can see that the results obtained within the framework of the massive field theory are situated slightly closer to experimental data. But this shift is not enough in order to obtain good quantitative agreement with the experiment. One of the possible ways to find a good agreement could be connected with further theoretical investigation of crossover region from wide to narrow slit and taking into account additional corrections to the Derjaguin approximation.

We gratefully acknowledge fruitful discussions with H.W. Diehl. This work in part was supported by grant from the Alexander von Humboldt Foundation (Z.U.).

APPENDIX A: THE FREE PROPAGATORS FOR DIFFERENT BOUNDARY CONDITIONS

In the case of Dirichlet-Dirichlet boundary conditions $c_1/m\to\infty$ and $c_2/m\to\infty$ the free propagator in the slit geometry has a form

$$\tilde{G}_{\parallel}^{D,D}(\mathbf{p},z,z';\mu_0,L)=\frac{1}{2\kappa}(e^{\kappa L}-e^{-\kappa L})^{-1}(e^{\kappa(L-|z-z'|)}+e^{-\kappa(L-|z-z'|)}-e^{\kappa(L-z-z')}-e^{-\kappa(L-z-z')}), \tag{A1}$$

and the corresponding half-space Dirichlet propagator is

$$\tilde{G}_{HS}^{D}(\mathbf{p},z,z';\mu_0)=\frac{1}{2\kappa}(e^{-\kappa|z-z'|}-e^{-\kappa(z+z')}). \tag{A2}$$

In the case of Neumann-Neumann boundary conditions $c_1/m\to 0$ and $c_2/m\to 0$ the free propagator in the slit geometry is written as

$$\tilde{G}_{\parallel}^{N,N}(\mathbf{p},z,z';\mu_0,L)=\frac{1}{2\kappa}(e^{\kappa L}-e^{-\kappa L})^{-1}(e^{\kappa(L-|z-z'|)}+e^{-\kappa(L-|z-z'|)}+e^{\kappa(L-z-z')}+e^{-\kappa(L-z-z')}), \tag{A3}$$

and the corresponding half-space Neumann propagator is

$$\tilde{G}_{HS}^{N}(\mathbf{p},z,z';\mu_0)=\frac{1}{2\kappa}(e^{-\kappa|z-z'|}+e^{-\kappa(z+z')}). \tag{A4}$$

The free propagator for the mixed Dirichlet-Neumann boundary conditions $c_1/m\to\infty$ and $c_2/m\to 0$ in the slit geometry has a form

$$\tilde{G}_{\parallel}^{D,D}(\mathbf{p},z,z';\mu_0,L)=\frac{1}{2\kappa}(e^{\kappa L}+e^{-\kappa L})^{-1}(e^{\kappa(L-|z-z'|)}-e^{-\kappa(L-|z-z'|)}+e^{\kappa(L-z-z')}-e^{\kappa(L-z-z')}). \tag{A5}$$

APPENDIX B: THE SURFACE CONTRIBUTIONS

To calculate the function Υ defined in Eq. (3.13), we need the free propagator for a semi-infinite system confined by a surface at $z=0$. This free full propagator has form [17]

$$\tilde{G}_{ijHS}^{(2)}(\mathbf{p},\mathbf{p}',z,z';\mu_0,c_0)=(2\pi)^{d-1}\delta_{ij}\delta(\mathbf{p}+\mathbf{p}')\tilde{G}_{HS}(\mathbf{p},z,z',\mu_0,c_0), \tag{B1}$$

with

$$\tilde{G}_{HS}(\mathbf{p},z,z',\mu_0,c_0):=\frac{1}{2\kappa_0}\left(e^{-\kappa_0|z-z'|}+\frac{\kappa_0-c_0}{\kappa_0+c_0}\mathrm{e}^{-\kappa_0(z+z')}\right), \tag{B2}$$

where $\kappa_0=\sqrt{p^2+\mu_0^2}$.

In the zero-loop order we have

$$\Upsilon_i=\frac{1}{\mu^3}\frac{c_i}{\mu+c_i}. \tag{B3}$$

In one-loop order the calculation for Dirichlet boundary conditions on the surface (or $\frac{c}{m}\to\infty$) yields after renormalization in fixed dimensions $d=3$

$$\Upsilon^{D}=\frac{1}{\mu^3}\left(1-\frac{n+2}{n+8}\tilde{v}\ln\frac{9}{8}\right). \tag{B4}$$

And for Neumann boundary conditions ($c=0$) after renormalization we obtain

$$\Upsilon^{N}=\frac{\tilde{v}}{\mu^3}\left(\ln 2-\frac{1}{2}\right)\frac{n+2}{n+8}, \tag{B5}$$

where we introduced rescaled renormalized coupling constant $\tilde{v}$ in the form $\tilde{v}=\frac{(n+8)}{6}\frac{\Gamma(\epsilon/2)}{(4\pi)^{d/2}}v$. The correspondent fixed point in one-loop order approximation is $\tilde{v}^*=1$.

APPENDIX C: THE CASE OF FINITE SLIT SEPARATION FOR TWO INERT WALLS

Taking into account the new δc_i^{S-S} [see Eq. (4.9)] we can calculate δf in accordance with Eq. (6.12) for the case of big but finite slit separation L. We obtain

$$\delta f\approx\mathcal{IL}_{\mu^2\to R_x^2/2}\left(\frac{2\Delta^{(S-S)}}{\mu^4}+\frac{e^{-2\mu L}}{2\mu^3}\right). \tag{C1}$$

After substitution of $\Delta^{(S-S)}$ from Eq. (4.10) the result for δf is

$$\delta f\approx-\mathcal{IL}_{\mu^2\to R_x^2/2}\left\{\left(\frac{1}{\mu L}+C_E+7\ln 2-6+\ln\mu L-e^{4\mu L}\mathrm{Ei}(-4\mu L)\right)\frac{e^{-2\mu L}}{2\mu^3}\right\}. \tag{C2}$$

If we carry out the inverse Laplace transform, the result for $\Theta(y)$ in the wide slit limit is

$$\Theta(y)\approx-\frac{C_E+7\ln 2-7}{2}\left(\sqrt{\frac{2}{\pi}}e^{-2y^2}-2y\,\mathrm{erfc}(\sqrt{2}y)\right)-\frac{1}{4y}\mathrm{erfc}(\sqrt{2}y)-\frac{y}{4}\mathcal{IL}_{\tau\to 1/2y^2}\left(\frac{e^{-2\sqrt{\tau}}}{\tau^{3/2}}\ln\tau\right)+\frac{y}{2}\mathcal{IL}_{\tau\to 1/2y^2}\left(\frac{e^{2\sqrt{\tau}}}{\tau^{3/2}}\mathrm{Ei}(-4\sqrt{\tau})\right). \tag{C3}$$

In contrast to Eq. (6.11), this expression is indeed negative. Thus, if we perform calculations for the depletion interaction potential and the depletion force including big but finite slit separation L we obtain that force in the case of two inert walls changes character and becomes attractive. In Fig. 3 the depletion interaction potential and the depletion force obtained in the framework of this alternative renormalization scheme with δc_{slit} are plotted in comparison with the results obtained via the original renormalization using δc_{semi}. Here we introduced for convenience the following notations: $\delta c_{semi}=\delta c_i$ and $\delta c_i^{S-S}=\delta c_{slit}$ with $i=1,2$.

[1] H. B. G. Casimir, Proc. K. Ned. Acad. Wet. **51**, 793 (1948).
[2] M. E. Fisher and P. G. de Gennes, C. R. Acad. Sci. Ser. B **287**, 207 (1978).
[3] C. Hertlein, L. Helden, A. Gambassi, S. Dietrich, and C. Bechinger, Nature (London) **451**, 172 (2008).
[4] Y. N. Ohshima, H. Sakagami, K. Okumoto, A. Tokoyoda, T. Igarashi, K. B. Shintaku, S. Toride, H. Sekino, K. Kabuto, and I. Nishio, Phys. Rev. Lett. **78**, 3963 (1997).
[5] D. Rudhardt, C. Bechinger, and P. Leiderer, Phys. Rev. Lett. **81**, 1330 (1998).
[6] R. Verma, J. C. Crocker, T. C. Lubensky, and A. G. Yodh, Phys. Rev. Lett. **81**, 4004 (1998).
[7] B. V. Derjaguin, Kolloid-Z. **69**, 155 (1934).
[8] S. Asakura and F. Oosawa, J. Chem. Phys. **22**, 1255 (1954).
[9] S. Asakura and F. Oosawa, J. Polym. Sci. **33**, 183 (1958).
[10] J. F. Joanny, L. Leibler, and P. G. de Gennes, J. Polym. Sci., Polym. Phys. Ed. **17**, 1073 (1979).
[11] P. G. de Gennes, C. R. Seances Acad. Sci., Ser. B **288**, 359 (1979).
[12] T. Odijk, Macromolecules **29**, 1842 (1996); J. Chem. Phys. **106**, 3402 (1997).
[13] E. Eisenriegler, Phys. Rev. E **55**, 3116 (1997).
[14] F. Schlesener, A. Hanke, R. Klimpel, and S. Dietrich, Phys. Rev. E **63**, 041803 (2001).
[15] G. Parisi, J. Stat. Phys. **23**, 49 (1980).
[16] G. Parisi, *Statistical Field Theory* (Addison-Wesley, Redwood City, 1988).
[17] H. W. Diehl and M. Shpot, Nucl. Phys. B **528**, 595 (1998).
[18] Z. Usatenko, J. Stat. Mech.: Theory Exp. (2006) P03009.
[19] A. Milchev and K. Binder, Eur. Phys. J. B **3**, 477 (1998); **13**, 607 (2000).
[20] H.-P. Hsu and P. Grasberger, J. Chem. Phys. **120**, 2034 (2004).
[21] J. des Cloizeaux and G. Jannink, *Polymers in Solution* (Clarendon Press, Oxford, 1990).
[22] L. Schäfer, *Excluded Volume Effects in Polymer Solutions as Explained by the Renormalization Group* (Springer, Heidelberg, 1998).
[23] P. G. de Gennes, Phys. Lett. A **38**, 339 (1972); *Scaling Concepts in Polymer Physics* (Cornell University Press, Ithaca, NY, 1979).
[24] H. W. Diehl and S. Dietrich, Z. Phys. B **42**, 65 (1981).
[25] H. W. Diehl, in *Phase Transitions and Critical Phenomena*, edited by C. Domb and J. L. Lebowitz (Academic Press, London, 1986), Vol. 10, pp. 75–267.
[26] E. Eisenriegler, *Polymers Near Surfaces* (World Scientific, Singapore, 1993).
[27] M. Krech and S. Dietrich, Phys. Rev. A **46**, 1886 (1992).
[28] E. Brézin, J. C. Le Guillou, and J. Zinn-Justin, in *Phase Transitions and Critical Phenomena*, edited by C. Domb and M. S. Green (Academic Press, London, 1976), Vol. 6, p. 125.
[29] D. J. Amit, *Field Theory, The Renormalization Group and Critical Phenomena* (World Scientific, Singapore, 1984).
[30] J. Zinn-Justin, *Euclidean Field Theory and Critical Phenomena* (Oxford University Press, New York, 1989).
[31] C. Itzykson and J.-M. Drouffe, *Statistical Field Theory* (Cambridge University Press, Cambridge, 1989), Vol. 1.
[32] I. S. Gradshteyn and I. M. Ryzhik, *Table of Integrals, Series, and Products* (Elsevier, New York, 2007).
[33] D. Grüneberg and H. W. Diehl, Phys. Rev. B **77**, 115409 (2008).